

Optimal robust detection statistics for pulsar timing arraysRUTGER VAN HAASTEREN,¹ BRUCE ALLEN,¹ AND JOSEPH D. ROMANO²¹*Max-Planck-Institut für Gravitationsphysik (Albert-Einstein-Institut), Callinstraße 38, D-30167 Hannover, Germany
Leibniz Universität Hannover, D-30167 Hannover, Germany*²*Department of Physics and Astronomy, University of Texas Rio Grande Valley,
One West University Boulevard, Brownsville, TX 78520, USA***ABSTRACT**

Pulsar timing arrays (PTAs) seek to detect a nano-Hz stochastic gravitational-wave background (GWB) by searching for the characteristic Hellings and Downs angular pattern of timing residual correlations. So far, the evidence remains below the conventional $5\text{-}\sigma$ threshold, as assessed using the literature-standard “optimal cross-correlation detection statistic”. While this quadratic combination of cross-correlated data maximizes the *deflection* (signal-to-noise ratio), it does not maximize the detection probability at fixed false-alarm probability (FAP), and therefore is not Neyman-Pearson (NP) optimal for the assumed noise and signal models. The NP-optimal detection statistic is a different quadratic form, but is not used because it also incorporates autocorrelations, making it more susceptible to uncertainties in the modeling of pulsar timing noise. Here, we derive the best compromise: a quadratic detection statistic which is as close as possible to the NP-optimal detection statistic (minimizing the variance of its difference with the NP statistic) subject to the constraint that it only uses cross-correlations, so that it is less affected by pulsar noise modeling errors. We study the performance of this new NPMV statistic for a simulated PTA whose noise and (putative) signal match those of the NANOGrav 15-year data release: GWB amplitude $A_{\text{gw}} = 2.1 \times 10^{-15}$ and spectral index $\gamma = 13/3$. Compared to the literature-standard “optimal” cross-correlation detection statistic, the NPMV statistic increases the detection probability by 47% when operating at a $5\text{-}\sigma$ FAP of $\alpha = 2.9 \times 10^{-7}$.

Keywords: gravitational waves — methods: data analysis — methods: statistical — pulsars: general — stars: neutron

1. INTRODUCTION

Four pulsar timing array (PTA) collaborations have reported evidence for a nano-Hz gravitational-wave background (GWB) (Agazie et al. 2023a; Reardon et al. 2023; Antoniadis et al. 2023; Xu et al. 2023). The time of arrival fluctuations from the pulsars that they monitor display a characteristic pattern of angular correlations among different pulsars, first predicted by Hellings & Downs (HD) (Hellings & Downs 1983; Allen 2023). One potential source for this GWB is a population of supermassive black-hole binaries at the centers

of galaxies (Agazie et al. 2023b; Antoniadis et al. 2024a,b). Other, more exotic sources have also been proposed and studied (Afzal et al. 2023).

While they have exhibited several types of evidence in favor of the GWB, none of the PTAs has made a detection claim. To do so, PTAs must demonstrate that their data are consistent with the HD pattern with at least a $5\text{-}\sigma$ -equivalent false-alarm probability (FAP) (Allen et al. 2023). For this purpose, the PTA community has adopted the so-called “optimal cross-correlation detection statistic” (Anholm et al. 2009; Chamberlin et al. 2015; Vigeland et al. 2018; Allen & Romano 2023, 2024). Here, we call this the *cross-correlation deflection* statistic, indicated with the subscript “DFCC”.

The cross-correlation deflection statistic is an example of a quadratic *detection statistic* (also known as a *test statistic*)

bruce.allen@aei.mpg.de

joseph.romano@utrgv.edu

Corresponding author: Rutger van Haasteren
rutger@vhaasteren.com

defined by the quadratic form

$$D(z|\mathbf{Q}) \equiv z^\dagger \mathbf{Q} z. \quad (1)$$

Here, z denotes the data (a complex column vector of dimension n , with \dagger denoting complex-conjugate transpose) and \mathbf{Q} denotes the *filter* (or *kernel*) of the quadratic form, which is a Hermitian matrix. From here forward, we will call D a “statistic” and \mathbf{Q} a “filter”.

In general, a detection statistic can be an *arbitrary* function of the data, $D \equiv D(z)$: those defined by a quadratic form (1) are thus a restricted class of detection statistics. In what follows, we will omit the argument \mathbf{Q} from the statistic if a statement or definition that we make applies to a general detection statistic. To emphasize that a particular formula or definition is specific to quadratic detection statistics, then we will include the argument \mathbf{Q} as in $D(z|\mathbf{Q})$.

In the simplest model, the dimension of z is the number of pulsars, and each component of z is the complex Fourier amplitude of the timing residual for that pulsar at one frequency. In more realistic models, z has several complex Fourier amplitudes per pulsar, typically grouped together by pulsar.

A detection statistic $D(z)$ together with a real *threshold* τ define a *decision rule* for either accepting or rejecting the null hypothesis H_0 . If $D(z) < \tau$ then H_0 is accepted: no GWB was found. If $D(z) > \tau$ then H_0 is rejected: a GWB was detected. The threshold τ is selected so that the probability α of claiming detection of a GWB when no GWB was present has a small value, e.g., $\alpha = 2.9 \times 10^{-7}$ for 5- σ (Gaussian-equivalent) significance.

The null hypothesis H_0 is equivalent to providing a probability distribution $P_0(z) \equiv P(z|H_0)$ on the data z . That allows us to define ensemble averages (or expectation values) of functions $f(z)$:

$$\langle f(z) \rangle_{H_0} \equiv \int d^n z f(z) P_0(z). \quad (2)$$

We will also make use of a *signal hypothesis* H_S with its corresponding probability distribution $P_S(z) \equiv P(z|H_S)$. Expected values with respect to that probability distribution are given by (2) with H_0 replaced by H_S and P_0 replaced by P_S .

The *false alarm probability* (FAP) α is the probability of the detection statistic exceeding the detection threshold τ in the *absence* of a GWB signal. It is

$$\alpha \equiv \text{Prob}(D > \tau | H_0) \equiv \langle \theta(D(z) - \tau) \rangle_{H_0}, \quad (3)$$

where $\theta(x)$ is the Heaviside step function defined after (40). The *detection probability* $\text{DP} \equiv 1 - \beta$ is similarly defined:

$$\text{DP} \equiv 1 - \beta \equiv \text{Prob}(D > \tau | H_S) \equiv \langle \theta(D(z) - \tau) \rangle_{H_S}, \quad (4)$$

where the expected value uses the signal hypothesis H_S . DP is the probability of the detection statistic exceeding the

threshold τ in the *presence* of a GWB signal, and β is the *false dismissal probability*.

The filter \mathbf{Q} for the general deflection statistic is chosen to maximize the ratio of the square of the difference of the expected values of $D(z|\mathbf{Q})$ under the signal and noise hypotheses H_S and H_0 , respectively, to its variance under H_0 : this is the sense in which it is “optimal”. Surprisingly, even for the case of two simple hypotheses (models with no free parameters¹), the deflection-optimal statistic is *not* the Uniformly Most Powerful (UMP) test.

Among all possible statistics [arbitrary functions $D(z)$] the UMP test is guaranteed to maximize the detection probability at fixed FAP. It may be obtained via the Neyman-Pearson (NP) Lemma, and is any monotonic function of the ratio of the probability distributions defining H_S and H_0 , see (9). If, as in this paper, H_S and H_0 are multivariate zero-mean Gaussian distributions, then the statistic is a quadratic form as in (1), see (10). In this paper, the UMP statistic and corresponding filter are indicated with the subscript “NP”. They are not the same as (or proportional to, or monotonic functions of) the DFCC statistic and corresponding filter.

Why has the PTA community chosen to adopt a statistic (DFCC) which is not the most powerful one? The reason is that the DFCC statistic depends only upon pulsar timing residual cross-correlations, and not upon pulsar timing residual autocorrelations, whereas the NP statistic depends upon *both*. That is undesirable, because it makes the NP statistic more vulnerable to errors arising from modeling of the (non-GWB) pulsar noise. To indicate this weakness, we say that the NP statistic is *not robust*.

In this paper, we exploit the gap between the DFCC and NP statistics. We construct a quadratic statistic, whose performance lies in between NP and DFCC, but which is robust. More precisely, we find the filter \mathbf{Q} whose quadratic statistic (1) is as close as possible (in the minimum-variance sense) to the NP statistic under the null hypothesis, but which is robust because it does not use auto-correlations. This corresponds to filters \mathbf{Q} which vanish on the diagonal. At a given FAP, we will see that the detection probability for this “Neyman-Pearson-Minimum-Variance” (NPMV) statistic is higher than that of the conventional DFCC statistic.

We employ a standard technique to characterize and compare different statistics: via their receiver operating characteristic (ROC) curves (see Secs. 7.2 and 7.3). These plot the detection probability as a function of FAP. We use these to show that in realistic cases the NPMV statistic has better performance (larger area under the ROC curve) than the standard DFCC statistic. For a PTA similar to the published

¹ In practice, for composite hypotheses (models with free parameters), these statistics are still used (Agazie et al. 2024; Vallisneri et al. 2023; van Haasteren 2025).

NANOGrav 15-year dataset, the NPMV statistic increases the detection probability by $\sim 47\%$ when operating at the $5\text{-}\sigma$ detection threshold FAP of 2.9×10^{-7} (see Fig. 3).

Given its improved performance, we believe that the NPMV detection statistic should replace the (currently standard) “optimal” cross-correlation statistic for evaluating detection claims and p -values in PTA data analysis.² At a given FAP, the NPMV statistic achieves higher detection probability while remaining robust to pulsar noise modeling errors.

To encourage its adoption, we provide a Python implementation of the NPMV filter and statistic in the `enterprise_extensions` package (Ellis et al. 2020; Taylor et al. 2021).

2. AUTOCORRELATIONS AND CROSS-CORRELATIONS

To facilitate discussion of auto- and cross-correlations, assume (without loss of generality) that the vector z of data is *grouped by pulsar*. This means that the first m_1 components are data from pulsar 1, the next m_2 components are data from pulsar 2, and so on. For each given pulsar, these data might be Fourier amplitudes at different frequencies, or different amplitudes in a Legendre polynomial decomposition, or timing residuals measured at different epochs.

Matrices such as the covariance Σ , whose rows and columns carry the same indices as z , may then be described as being composed of *blocks*. These blocks are delineated by drawing vertical lines between any neighboring columns associated with different pulsars, and by drawing horizontal lines between any neighboring rows associated with different pulsars.

The *block diagonal* of such a matrix consists of those *blocks* containing at least one diagonal element of the matrix.

For such a matrix \mathbf{M} , we define a linear operator `Diag` as follows: `Diag M` is the matrix obtained from \mathbf{M} by zeroing all entries that lie *off* the block diagonal. This differs from `diag M`, which is obtained from \mathbf{M} by setting all non-diagonal entries to zero. (If there is only one data sample per pulsar, then `Diag M` = `diag M`.) A matrix \mathbf{M} is said to be *block-diagonal* iff `Diag M` = \mathbf{M} .

From here forward, we will assume that the data vector z is grouped by pulsar. This means that the *diagonal blocks* of covariance matrices and quadratic filters contain autocorrelation terms. The remaining blocks, which contain cross-correlation terms, are called the *off-diagonal blocks*.

3. DEFINITIONS OF THE DETECTION STATISTICS

Here, we define the five different quadratic detection statistics (DF, DFCC, NP, NPCC, and NPMV) considered in this paper, and give formulas for four of the corresponding filters.

² The p -value for a detection statistic is defined as $p \equiv \text{Prob}(D > D_{\text{obs}} | H_0)$, where $D_{\text{obs}} \equiv D(z_{\text{obs}})$ for the observed data z_{obs} .

The NPMV filter is derived in Sec. 5 and derivations of the NP and DF filters are given in van Haasteren (2025).

In what follows, the null and signal hypotheses H_0 and H_S are assumed to be zero-mean multivariate Gaussian distributions for the complex-valued data z . These distributions are defined by the covariance matrices \mathbf{N} and \mathbf{C} , respectively, which are Hermitian and positive-definite. Later, starting in Sec. 4.1, we will restrict \mathbf{N} to the form most often used in PTA analyses. But here, \mathbf{N} and \mathbf{C} are *arbitrary* Hermitian, positive-definite matrices.

3.1. Quadratic filter definitions

As described in Sec. 1, the filter \mathbf{Q} for the general deflection-optimal statistic is defined by the requirement that it maximize the ratio of the square of the difference of the expected values of $D(z|\mathbf{Q})$ under H_S and H_0 , respectively, to its variance under H_0 . Thus,

$$\mathbf{Q}_{\text{DF}} \equiv \arg \max_{\mathbf{Q}} \frac{(\langle D(z|\mathbf{Q}) \rangle_{H_S} - \langle D(z|\mathbf{Q}) \rangle_{H_0})^2}{\text{Var}[D(z|\mathbf{Q})]_{H_0}}, \quad (5)$$

where the variance of (complex) w is

$$\text{Var}[w] \equiv \langle |w - \langle w \rangle|^2 \rangle = \langle |w|^2 \rangle - |\langle w \rangle|^2. \quad (6)$$

As shown by van Haasteren (2025), requirement (5) leads to:

$$\mathbf{Q}_{\text{DF}} = \mathbf{N}^{-1} (\mathbf{C} - \mathbf{N}) \mathbf{N}^{-1}. \quad (7)$$

For arbitrary covariance matrices \mathbf{N} and \mathbf{C} , \mathbf{Q}_{DF} does not vanish on the block diagonal, so in general it uses both auto- and cross-correlations. [For the PTA CURN null hypothesis, it only uses cross-correlations, see (14) and Sec. 4.1.]

A *robust* version of the deflection-optimal statistic, which uses only cross-correlations, can be derived in the same fashion as the general DF statistic. One first restricts the filter to use only cross-correlations, then maximizes, obtaining

$$\mathbf{Q}_{\text{DFCC}} = \mathbf{Q}_{\text{DF}} - \text{Diag } \mathbf{Q}_{\text{DF}}. \quad (8)$$

\mathbf{Q}_{DFCC} is the literature-standard “optimal cross-correlation detection statistic”, obtained from (7) by removing the auto-correlations from the general DF filter. It is used to search for GWBs with terrestrial GW detectors like LIGO, and for cross-correlation PTA analyses with non-standard null hypotheses, as discussed in Sec. 4.

Equation (7) does not include the usual data-independent normalization factor $(\text{Tr}[(\mathbf{N}^{-1}(\mathbf{C} - \mathbf{N}))^2])^{1/2}$ in the denominator of (7). This factor is usually inserted to ensure that the variance of \mathbf{Q}_{DF} is unity under H_0 . Here, however, we compare the performance of different detection statistics. This performance is encoded in the ROC curves, which give the detection probability as a function of the FAP, and are independent of the filter normalization.

As discussed in Sec. 1, the NP-optimal statistic maximizes the detection probability for a given FAP,

$$D_{\text{NP}} \equiv \arg \max_{D \mid \text{Prob}(D > \tau | H_0) = \alpha} \text{Prob}(D > \tau | H_S). \quad (9)$$

It is proportional to the log-likelihood ratio $\log P(z|H_S) - \log P(z|H_0) = \log(P_S(z)/P_0(z))$. In general, this quantity is not a quadratic function of z . However, for our specific choices of multivariate zero-mean Gaussian distributions for H_0 and H_S , it is quadratic, with filter

$$\mathbf{Q}_{\text{NP}} \equiv \mathbf{N}^{-1} - \mathbf{C}^{-1}. \quad (10)$$

As before, this could be normalized by dividing by a factor of $(\text{Tr}[(\mathbf{C}^{-1}(\mathbf{C} - \mathbf{N}))^2])^{1/2}$, but this serves no purpose here. Interestingly, in the limit of weak GWB signals (relative to the noise, meaning $\mathbf{C} \approx \mathbf{N}$), \mathbf{Q}_{NP} reduces to \mathbf{Q}_{DF} .

While the NP filter in (10) is the best possible detection statistic (in the Neyman-Pearson UMP sense), it is not used in practice in the PTA community because $\text{Diag } \mathbf{Q}_{\text{NP}} \neq 0$. This means that the detection statistic incorporates autocorrelations, which in turn are subject to pulsar noise mismodeling uncertainties. To obtain a robust version of the NP-optimal test, we first sought a statistic that maximizes the detection probability at fixed FAP, subject to the constraint that it does not use autocorrelation information. However, if the number of pulsars is ≥ 3 , then no such statistic exists, because the autocorrelations can be reconstructed from the cross-correlations.

We then sought a statistic that was quadratic in the data, of the form $D(z | \mathbf{Q})$ given in (1), with a filter \mathbf{Q} selected to maximize the detection probability at fixed FAP, subject to the constraint that $\text{Diag } \mathbf{Q} = 0$, so that the statistic uses only cross-correlations. We denote this filter by \mathbf{Q}_{NPCC} , but we were not able to obtain an analytic closed form for it. It can be found numerically (see Sec. 7.2) but the form of the solution (meaning its matrix “shape”, not just the overall normalization) depends upon the FAP, which makes it cumbersome to characterize and employ.

The NPMV statistic is a compromise between the cross-correlation-only deflection-optimal statistic DFCC and the auto+cross-correlation Neyman-Pearson-optimal statistic NP. By definition, it is “as close as possible” to the NP statistic, while using only cross-correlated data. More precisely, it minimizes the variance (MV) under H_0 of its difference with the NP statistic, subject to the constraint that the filter \mathbf{Q} vanish on the block diagonal:

$$\mathbf{Q}_{\text{NPMV}} \equiv \arg \min_{\mathbf{Q} \mid \text{Diag } \mathbf{Q} = 0} \text{Var}[D(z | \mathbf{Q}) - D(z | \mathbf{Q}_{\text{NP}})]_{H_0}. \quad (11)$$

For arbitrary \mathbf{N} , \mathbf{Q}_{NPMV} has a unique solution determined by (11) (see Sec. 5), but it does not have a very simple form. However, for block-diagonal \mathbf{N} , the unique solution is

$$\mathbf{Q}_{\text{NPMV}} = \mathbf{Q}_{\text{NP}} - \text{Diag } \mathbf{Q}_{\text{NP}} \quad (\text{assuming } \mathbf{N} = \text{Diag } \mathbf{N}). \quad (12)$$

This corresponds to simply removing the autocorrelation terms from the full NP-optimal filter. See Sec. 5 for a derivation of this relation.

With this in mind, the NPMV statistic can be thought of as the *bronze medalist*: it ranks third overall, after NP and NPCC. However, as we show in Sec. 7, the NPMV statistic significantly outperforms the DFCC statistic. A set of ROC curves, comparing NP, NPCC, NPMV, and DFCC for a simple model³ is presented in Sec. 7.2, Fig. 2.

4. NULL AND SIGNAL HYPOTHESES

In the previous section, the noise and signal hypotheses H_0 and H_S were defined by arbitrary Hermitian, positive-definite matrices \mathbf{N} and \mathbf{C} . However, conventional PTA analyses use hypotheses H_0 and H_S that make certain assumptions regarding the properties of the pulsars and the GW signals. These restrict the form of \mathbf{N} and \mathbf{C} . In this section, we describe some of these restricted forms of \mathbf{N} and \mathbf{C} , as we need this to understand how to apply our proposed methods to realistic PTA data.

4.1. Block-diagonal and CURN null hypotheses

For most stochastic background analyses, including GWB searches using ground-, space-, and galactic-based detectors like LIGO, LISA, and PTAs, the null hypothesis H_0 is defined by a *block-diagonal* covariance matrix \mathbf{N} :

$$\mathbf{N} = \text{Diag } \mathbf{N}. \quad (13)$$

This means that “detector noise” is uncorrelated between different detectors, or in the case of PTAs, between different pulsars.

It is also typical in PTA analyses to set the null hypothesis covariance \mathbf{N} to agree with the signal covariance matrix \mathbf{C} on the block diagonal:

$$\mathbf{N} = \text{Diag } (\mathbf{C}). \quad (14)$$

This H_0 is called the CURN hypothesis, meaning “common uncorrelated red noise”; see Sec. 4.2 of Ellis et al. (2013) where this choice of null hypothesis was first introduced. With this choice, the signal hypothesis H_S differs from the null hypothesis H_0 only via the effects of the off-diagonal blocks of \mathbf{C} . These off-diagonal blocks contain information about the Hellings and Downs (HD) cross-correlations induced by the GWB.

CURN is a conservative choice of H_0 . Rather than saying “there is no GWB”, it says “there is a background, but not of the type described by the general theory of relativity (GR)”. The CURN background contains common-spectrum autocorrelations in pulsar timing fluctuations, but without the

³ For this model, DF and DFCC are identical.

HD cross-correlations of GR. If the null hypothesis were “no GWB”, then the diagonal blocks of \mathbf{C} would contain *additional* contributions from the GWB that are not present in \mathbf{N} . Choosing CURN as H_0 makes the analysis less sensitive to pulsar noise modeling errors but also makes it less sensitive to the GWB. Hence, it is more conservative than the alternative of a “no GWB” H_0 .

One consequence of taking H_0 to be CURN is that the DF-optimal filter \mathbf{Q}_{DF} given in (7) involves only cross-correlations, thus implying $\mathbf{Q}_{\text{DF}} = \mathbf{Q}_{\text{DFCC}}$ for CURN.

4.2. Relating DF and NP filters for realistic PTA data

Realistic PTA data consists of multiple samples per pulsar. These data may be modeled using Gaussian processes (Rasmussen & Williams 2006; van Haasteren & Vallisneri 2014). For computational efficiency, realistic analyses use reduced-rank representations for the model components, obtained via a chain of basis transformations that whiten (see below) and reduce the dimension of the original data (van Haasteren 2025). Current analysis codes already compute the standard DF and DFCC filters in that reduced-dimension whitened basis. Here, we show how the suitably whitened NPMV filter may be directly obtained from the whitened DF filter for a block-diagonal noise hypothesis H_0 .

The whitened data are given by

$$\tilde{z} \equiv \mathbf{N}^{-1/2} z. \quad (15)$$

These are said to be “whitened” because the covariance matrix of \tilde{z} is the identity matrix \mathbf{I} . The whitening filter $\mathbf{N}^{-1/2}$ is well defined, because (as described above, and also true in the reduced basis) \mathbf{N} is block diagonal, with each block being Hermitian and positive-definite.

Under this whitening change of basis, detection statistics are invariant. For the quadratic detection statistics considered in this paper, this means that

$$D(z | \mathbf{Q}) = z^\dagger \mathbf{Q} z = D(\tilde{z} | \tilde{\mathbf{Q}}) = \tilde{z}^\dagger \tilde{\mathbf{Q}} \tilde{z}. \quad (16)$$

Substituting (15) into (16), we see that the whitened version of the filter \mathbf{Q} is given by

$$\tilde{\mathbf{Q}} \equiv \mathbf{N}^{1/2} \mathbf{Q} \mathbf{N}^{1/2}. \quad (17)$$

In this way, we use a \sim to denote both whitened data and whitened filters.

From (17), the whitened version of the DF filter (7) is

$$\tilde{\mathbf{Q}}_{\text{DF}} \equiv \mathbf{N}^{1/2} \mathbf{Q}_{\text{DF}} \mathbf{N}^{1/2} = \mathbf{A} - \mathbf{I}, \quad (18)$$

where \mathbf{I} is the identity matrix, and

$$\mathbf{A} \equiv \mathbf{N}^{-1/2} \mathbf{C} \mathbf{N}^{-1/2} \quad (19)$$

is the inverse of the whitened inverse-signal covariance $\mathbf{N}^{1/2} \mathbf{C}^{-1} \mathbf{N}^{1/2}$. From (17), the whitened version of the NP filter (10) is

$$\begin{aligned} \tilde{\mathbf{Q}}_{\text{NP}} &\equiv \mathbf{N}^{1/2} \mathbf{Q}_{\text{NP}} \mathbf{N}^{1/2} = \mathbf{I} - \mathbf{A}^{-1} \\ &= (\mathbf{A} - \mathbf{I}) \mathbf{A}^{-1} = \tilde{\mathbf{Q}}_{\text{DF}} (\mathbf{I} + \tilde{\mathbf{Q}}_{\text{DF}})^{-1}, \end{aligned} \quad (20)$$

where the final equality follows from (18). This means that the whitened NP filter can be easily constructed from the whitened DF filter.

From the whitened NP filter, it is easy to construct the whitened NPMV filter by removing the diagonal blocks:

$$\tilde{\mathbf{Q}}_{\text{NPMV}} = \tilde{\mathbf{Q}}_{\text{NP}} - \text{Diag } \tilde{\mathbf{Q}}_{\text{NP}}. \quad (21)$$

Since $\mathbf{N}^{1/2}$ is block-diagonal, this again corresponds to setting the diagonal blocks of the whitened NP-optimal filter to zero.

In a more realistic setting, this still works. Since $\tilde{\mathbf{Q}}_{\text{DF}}$ and $\mathbf{I} + \tilde{\mathbf{Q}}_{\text{DF}}$ commute, they share a common set of eigenvectors and they can be expressed in the same reduced basis. Therefore, these expressions hold for the compressed whitened data presented in van Haasteren (2025). This makes it straightforward to compute the NPMV filter and p -values with minimal modifications to existing codes.

5. DERIVATION OF THE NPMV FILTER

In this section, we derive the form of the NPMV filter defined by (11). For notational simplicity, we will assume in this section that the data z have only a single sample per pulsar, $z = \{z_a\}$, where $a = 1, 2, \dots, n$ runs over the number of pulsars in the array. Nonetheless, the results hold for the more general multi-sample case.

For most of this section, \mathbf{N} is an arbitrary Hermitian, positive-definite matrix. However, at the end, we restrict attention to block-diagonal \mathbf{N} as defined by (13). This assumption is needed to obtain the simple form of \mathbf{Q}_{NPMV} given in (12).

The NPMV detection statistic is defined by (11): D_{NPMV} is the quadratic form whose difference with D_{NP} has the smallest possible variance under H_0 , subject to the constraint that the filter \mathbf{Q}_{NPMV} does not use autocorrelations. Thus, \mathbf{Q}_{NPMV} minimizes

$$V(\mathbf{Q}) \equiv \text{Var}[D(z|\mathbf{Q}) - D(z|\mathbf{Q}_{\text{NP}})]_{H_0} \quad (22)$$

subject to the constraint

$$\text{Diag } \mathbf{Q} = 0 \iff Q_{aa} = 0, \quad (23)$$

where the pulsar index a is not summed. To simplify the expressions that follow, we define

$$\mathbf{\Lambda} \equiv \mathbf{Q} - \mathbf{Q}_{\text{NP}}, \quad (24)$$

for which

$$V(\mathbf{Q}) = \text{Var}[D(z|\mathbf{\Lambda})]_{H_0}. \quad (25)$$

Expanding the variance of Δ in terms of the data z , we find:

$$\begin{aligned}
 V(\mathbf{Q}) &= \langle |D(z|\Delta)|^2 \rangle_{H_0} - |\langle D(z|\Delta) \rangle_{H_0}|^2 \\
 &= \sum_{a,b,c,d} \Delta_{ab} \Delta_{cd}^* \left(\langle z_a^* z_b z_c z_d^* \rangle_{H_0} - \langle z_a^* z_b \rangle_{H_0} \langle z_c z_d^* \rangle_{H_0} \right) \\
 &= \sum_{a,b,c,d} \Delta_{ab} \Delta_{cd}^* \langle z_a^* z_c \rangle_{H_0} \langle z_b z_d^* \rangle_{H_0} \\
 &= \sum_{a,b,c,d} \Delta_{ab} \Delta_{cd}^* N_{ac}^* N_{bd} = \text{Tr}(\Delta \mathbf{N} \Delta \mathbf{N}),
 \end{aligned} \tag{26}$$

where the third equality follows from Isserlis's theorem (Isserlis 1918), the fourth equality from $\langle z_a z_b^* \rangle_{H_0} \equiv N_{ab}$, and the fifth from the Hermitian property of \mathbf{N} and Δ .

We now use the method of Lagrange multipliers to solve the constrained optimization problem. We optimize

$$L(\Lambda, \mathbf{Q}) \equiv \text{Tr}(\Delta \mathbf{N} \Delta \mathbf{N}) - \sum_a \Lambda_a Q_{aa}, \tag{27}$$

where Λ_a are the Lagrange multipliers (one per diagonal element of \mathbf{Q}). Setting the variations of L wrt Λ_a and Q_{ab} equal to zero gives

$$\delta \Lambda_a : Q_{aa} = 0, \tag{28}$$

$$\delta Q_{ab} : 2 \sum_{c,d} N_{bd} \Delta_{dc} N_{ca} - \Lambda_a \delta_{ab} = 0. \tag{29}$$

The first equation is the constraint (23). To work with the second equation, we multiply it by the inverse matrices $(N^{-1})_{eb}$ on the left and $(N^{-1})_{af}$ on the right; the matrix multiplication sums over all values of a and b . The result can be rewritten as

$$\Delta_{ef} = \frac{1}{2} \sum_a (N^{-1})_{ea} \Lambda_a (N^{-1})_{af}, \tag{30}$$

or, equivalently,

$$Q_{ab} = Q_{ab}^{\text{NP}} + \frac{1}{2} \sum_c (N^{-1})_{ac} \Lambda_c (N^{-1})_{cb}, \tag{31}$$

where we have relabeled the indices in the last equation and used (24) to express Δ in terms of \mathbf{Q} and \mathbf{Q}_{NP} .

The equations for the desired filter $\mathbf{Q}_{\text{NPMV}} = Q_{ab}$ have a unique solution. To see this, consider the diagonal and off-diagonal components of (31). These can be written

$$0 = Q_{aa}^{\text{NP}} + \frac{1}{2} \sum_c (N^{-1})_{ac} \Lambda_c (N^{-1})_{ca}, \tag{32}$$

$$Q_{\bar{a}\bar{b}} = Q_{\bar{a}\bar{b}}^{\text{NP}} + \frac{1}{2} \sum_c (N^{-1})_{\bar{a}c} \Lambda_c (N^{-1})_{c\bar{b}}, \tag{33}$$

where barred indices range over $1, 2, \dots, n$, but must not equal one another. The diagonal equations (32) arise from the constraint $Q_{aa} = 0$. They relate the Lagrange multipliers Λ_a

to the diagonal components of \mathbf{Q}_{NP} and the noise covariance matrix \mathbf{N} , and are n linear equations in the n variables Λ_a . Since the linear transformation

$$F_{ac} \equiv (N^{-1})_{ac} (N^{-1})_{ca} = |(N^{-1})_{ac}|^2 \tag{34}$$

is invertible⁴ they provide a unique solution for Λ_a . Substituting these Λ_a into the rhs of (33) provides the unique solution for $Q_{\bar{a}\bar{b}}$. \mathbf{Q}_{NPMV} then follows immediately, since from (28) the remaining (diagonal) terms vanish.

This filter \mathbf{Q} does not have the simple form given in (12). To obtain (12), we need to additionally assume that \mathbf{N} is block-diagonal, which is a standard assumption for noise covariance matrices; see Sec. 4.1. Then $N_{ac} = N_a \delta_{ac}$, implying

$$F_{ac} = N_a^{-2} \delta_{ac}. \tag{35}$$

This immediately leads to

$$\Lambda_a = -2N_a^2 Q_{aa}^{\text{NP}} \tag{36}$$

as the solution to (32). It also implies that the second term on the rhs of (33) vanishes:

$$\sum_c (N^{-1})_{\bar{a}c} \Lambda_c (N^{-1})_{c\bar{b}} = N_{\bar{a}}^{-2} \Lambda_{\bar{a}} \delta_{\bar{a}\bar{b}} = 0. \tag{37}$$

The final equality follows from $\delta_{\bar{a}\bar{b}} = 0$ for $\bar{a} \neq \bar{b}$, independent of the solution for Λ_a . Thus, for block-diagonal \mathbf{N} , we see from (37) and (33) that

$$Q_{\bar{a}\bar{b}} = Q_{\bar{a}\bar{b}}^{\text{NP}}. \tag{38}$$

Then (28) and (38) give the full solution

$$Q_{aa}^{\text{NPMV}} = 0, \quad Q_{\bar{a}\bar{b}}^{\text{NPMV}} = Q_{\bar{a}\bar{b}}^{\text{NP}} \quad (\bar{a} \neq \bar{b}), \tag{39}$$

which may also be written as (12).

6. GENERALIZED χ^2 DISTRIBUTION

For a multivariate normal distribution, the detection and false-alarm probabilities associated with quadratic statistics (1) are described by generalized χ^2 distributions. A discussion of their cumulative distribution function (CDF), and their application to PTAs (for example, computing p -values) may be found in Hazboun et al. (2023). This also contains citations to the more general literature on this topic, for example Das & Geisler (2021).

The general case has a real data space, a normal distribution defined by a real positive-definite symmetric covariance matrix, and a statistic (1) defined by a real symmetric matrix

⁴ Since \mathbf{N} is Hermitian and positive-definite, this follows from the Schur product theorem (see Assertion (c) of (7.5.3) in Horn & Johnson (2012), with $\mathbf{A} = \mathbf{N}^{-1}$ and $\mathbf{B} = (\mathbf{N}^{-1})^*$).

(filter) \mathbf{Q} . For this general case, there is no known closed form for the CDF. However, there are many different algorithms and computer packages to evaluate it (Das & Geisler 2021).

The complex normal distribution of dimension n is a special case. It is equivalent to a real data space of dimension $2n$, where (in a suitable basis) the real random variables come in pairs (x_j, y_j) , where x_j and y_j are statistically independent of one another and have identical variance for $j = 1, \dots, n$. Then, the distribution of $x_j^2 + y_j^2$ is exponential, and the CDF factors into a product of exponentials. For this special case, an explicit closed form for the CDF is obtained (Cox 1962, pg. 17 Eq. (4)) using Laplace transforms.

Those results assume that the statistic $D(z|\mathbf{Q})$ given in (1) is positive or negative-definite. Here, we are interested in matrices (filters) \mathbf{Q} which vanish on the diagonal. Since $\text{Tr } \mathbf{Q} = 0$, it follows that \mathbf{Q} has eigenvalues of both signs. With this as motivation, we provide a derivation of the CDF for the indefinite case, which we use to characterize and optimize decision rules.

6.1. Definitions

Let z denote a complex column vector, \mathbf{C} a Hermitian positive-definite covariance matrix, and \mathbf{Q} a Hermitian matrix, all of dimension n . We assume that \mathbf{Q} has no vanishing eigenvalues: it is full rank.

The CDF for a generalized (central) χ^2 distribution with n complex degrees of freedom as given in (52) is

$$F(\tau, \mathbf{C}, \mathbf{Q}) \equiv \frac{1}{\det(2\pi\mathbf{C})} \int d^n z \theta(\tau - z^\dagger \mathbf{Q} z) e^{-\frac{1}{2} z^\dagger \mathbf{C}^{-1} z}. \quad (40)$$

This may also be written in the notation of (2) as $F(\tau, \mathbf{C}, \mathbf{Q}) = \langle \theta(\tau - z^\dagger \mathbf{Q} z) \rangle_{H_C} = 1 - \langle \theta(D(z|\mathbf{Q}) - \tau) \rangle_{H_C}$. The Heaviside step function $\theta(x) = 1$ for $x > 0$, $1/2$ for $x = 0$, and vanishes for $x < 0$. F is the probability that the quadratic form $D = z^\dagger \mathbf{Q} z$ is less than a real threshold τ ; F vanishes as $\tau \rightarrow -\infty$, and approaches 1 as $\tau \rightarrow +\infty$. For \mathbf{Q} positive (negative) definite, F has its support on the positive (negative) τ -axis. If \mathbf{Q} is indefinite, then F is nonzero for all τ .

In the space of possible data $z \in \mathbb{C}^n$, the normal distribution $\exp(-\frac{1}{2} z^\dagger \mathbf{C}^{-1} z)$ has level surfaces which are ellipsoids, with principal-axis directions and squared lengths given by the eigenvectors and eigenvalues of \mathbf{C} . The statistic $D = z^\dagger \mathbf{Q} z$ has level surfaces which are ellipsoids if \mathbf{Q} is positive or negative definite. If \mathbf{Q} has indefinite signature $(-, \dots, -, +, \dots, +)$, then the level surfaces are nested hyperbolic sheets.

6.2. Evaluation of F

To evaluate $F \equiv F(\tau, \mathbf{C}, \mathbf{Q})$, we first represent the Heaviside step function as the Fourier integral

$$\theta(x) = \lim_{\epsilon \rightarrow 0^+} \int_{-\infty}^{\infty} df \frac{e^{2\pi i f x}}{2\pi i (f - i\epsilon)}, \quad (41)$$

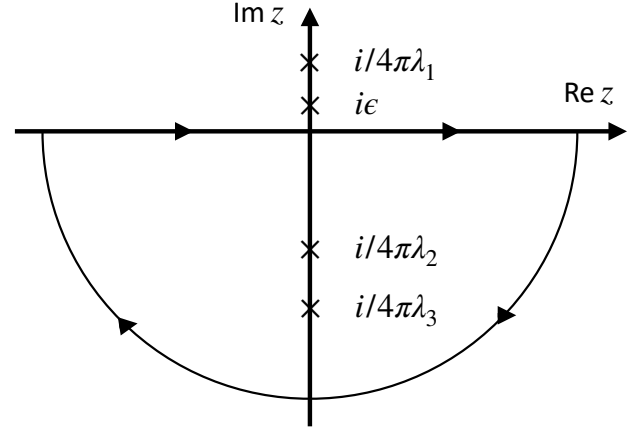


Figure 1. In the complex z -plane, the integrand of (45) is analytic apart from $n + 1$ poles along the imaginary axis. We illustrate the 3-dimensional case for which \mathbf{E} has one positive and two negative eigenvalues. If $\tau < 0$, the integral along the real axis is evaluated by closing the contour of integration in the lower half-plane, and using Cauchy's residue theorem.

where $\epsilon > 0$ is real. The derivative of (41) with respect to x yields the standard expression for the Dirac delta function.

One can verify (41) by inspection, using Cauchy's residue theorem. For $x < 0$, the exponential $e^{2\pi i f x}$ falls off exponentially as $f \rightarrow -i\infty$, so one can close the path of integration with a clockwise half circle in the lower half complex f -plane, similar to that shown in Fig. 1. Since the pole at $f = i\epsilon$ lies above the real axis, the contour of integration does not contain any poles, so the sum of the residues vanishes and $\theta(x) = 0$. For $x > 0$ one can close the path of integration with a counterclockwise half circle in the upper half complex f -plane. The residue of the pole is $1/2\pi i$, so the residue theorem gives $\theta(x) = 1$. For $\theta(0)$ take the principle value.

Substituting (41) into (40) gives

$$F = \lim_{\epsilon \rightarrow 0^+} \int_{-\infty}^{\infty} df \frac{e^{2\pi i f \tau}}{2\pi i (f - i\epsilon)} \int d^n z \frac{e^{-\frac{1}{2} z^\dagger [\mathbf{C}^{-1} + 4\pi i f \mathbf{Q}] z}}{\det(2\pi\mathbf{C})}. \quad (42)$$

The integral over z is easily evaluated, giving

$$\begin{aligned} F &= \lim_{\epsilon \rightarrow 0^+} \int_{-\infty}^{\infty} df \frac{e^{2\pi i f \tau}}{2\pi i (f - i\epsilon)} \frac{\det(2\pi [\mathbf{C}^{-1} + 4\pi i f \mathbf{Q}]^{-1})}{\det(2\pi\mathbf{C})} \\ &= \lim_{\epsilon \rightarrow 0^+} \int_{-\infty}^{\infty} df \frac{e^{2\pi i f \tau}}{2\pi i (f - i\epsilon)} \frac{1}{\det(\mathbf{I} + 4\pi i f \mathbf{E})}, \end{aligned} \quad (43)$$

where

$$\mathbf{E} \equiv \mathbf{C}^{1/2} \mathbf{Q} \mathbf{C}^{1/2}. \quad (44)$$

Here, $\mathbf{C}^{1/2}$ denotes the unique Hermitian, positive-definite matrix satisfying $\mathbf{C} = \mathbf{C}^{1/2} \mathbf{C}^{1/2}$.

Let λ_j for $j = 1, 2, \dots, n$ denote the (real) eigenvalues of the Hermitian matrix \mathbf{E} , which we assume are distinct (non-

degenerate). Then, since \mathbf{I} commutes with \mathbf{E} ,

$$F = \lim_{\epsilon \rightarrow 0^+} \int_{-\infty}^{\infty} \frac{dz}{2\pi i(z - i\epsilon)} \frac{e^{2\pi i \tau z}}{\prod_j (1 + 4\pi i \lambda_j z)} \quad (45)$$

$$= \frac{1}{\det(4\pi i \mathbf{E})} \lim_{\epsilon \rightarrow 0^+} \int_{-\infty}^{\infty} \frac{dz}{2\pi i(z - i\epsilon)} \frac{e^{2\pi i \tau z}}{\prod_j (z - z_j)}.$$

Here, we changed the name of the integration variable f to the complex variable $z = x + iy$ [not to be confused with the complex data vector z , which was integrated away in (42) to obtain (43)]. We also defined

$$z_j \equiv \frac{i}{4\pi \lambda_j}. \quad (46)$$

These are a set of n purely imaginary values determined by the eigenvalues of \mathbf{E} .

The integrand in (45) is a meromorphic function on the complex z -plane, which is holomorphic except at the isolated poles $z = z_j$ and $z = i\epsilon$ along the imaginary axis, as illustrated in Fig. 1. The numerator is analytic everywhere, and the denominator grows $\propto R^{n+1}$ for large $R \equiv |z|$. Hence, one can apply arguments identical to those following (41). For $\tau < 0$ we close the path of integration with a half-circle in the lower half z -plane which encloses all of the poles along the negative imaginary axis, as shown in Fig. 1. The sum of their residues gives the integral via Cauchy's theorem.

To simplify matters, first assume that one eigenvalue $\lambda_1 < 0$ of \mathbf{E} is negative, that the remaining eigenvalues are positive, that all of the eigenvalues are distinct, and that $\tau < 0$. Then, the integration contour encloses a single pole located at $z = z_1$, and Cauchy's residue theorem gives

$$F(\tau, \mathbf{C}, \mathbf{Q}) = \frac{-2\pi i}{\det(4\pi i \mathbf{E})} \frac{e^{2\pi i \tau z_1}}{2\pi i z_1 \prod_{j \neq 1} (z_1 - z_j)}, \quad (47)$$

where the minus sign is because the contour of integration is clockwise. Substituting (46) and canceling factors gives

$$F(\tau, \mathbf{C}, \mathbf{Q}) = e^{-\tau/2\lambda_1} \prod_{j \neq 1} \left(1 - \frac{\lambda_j}{\lambda_1}\right)^{-1} \text{ for } \tau < 0. \quad (48)$$

If there are multiple negative eigenvalues, then

$$F(\tau, \mathbf{C}, \mathbf{Q}) = \sum_{j|\lambda_j < 0} e^{-\tau/2\lambda_j} \prod_{k \neq j} \left(1 - \frac{\lambda_k}{\lambda_j}\right)^{-1} \text{ for } \tau < 0. \quad (49)$$

If there are no negative eigenvalues, then $F = 0$ for $\tau < 0$.

It is trivial to obtain F for $\tau > 0$. Since $\theta(x) = 1 - \theta(-x)$, it follows immediately from (40) that $F(\tau, \mathbf{C}, \mathbf{Q}) = 1 - F(-\tau, \mathbf{C}, -\mathbf{Q})$. Thus, for $\tau > 0$, (49) implies that

$$F(\tau, \mathbf{C}, \mathbf{Q}) = 1 - \sum_{j|\lambda_j > 0} e^{-\tau/2\lambda_j} \prod_{k \neq j} \left(1 - \frac{\lambda_k}{\lambda_j}\right)^{-1} \text{ for } \tau > 0. \quad (50)$$

If there are no positive eigenvalues, then $F = 1$ for $\tau > 0$. Note that the products in (49) and (50) include $n - 1$ terms.

A numerical issue called ‘‘catastrophic cancellation’’ makes (49) and (50) challenging to evaluate. The coefficients of the exponential terms typically range over $n = \dim \mathbf{E}$ (or more) orders of magnitude. In our one-frequency-bin example, the NPMV filter for $n = 67$ pulsars has 16 positive eigenvalues and 51 negative eigenvalues. For low FAP, we only need the 16 $\lambda_j > 0$ terms in (50). This is still possible in the precision provided by IEEE 754 doubles, which have a 53 bit mantissa. But high FAP calculations or larger numbers of dimensions require arbitrary precision libraries.

7. FILTER PERFORMANCE COMPARISON

Here, we use ROC curves to compare the performance of four different quadratic statistics of the form (1). The first is NP, which (by construction) has the best performance. Next is the (numerically-constructed) NPCC filter, which maximizes the detection probability at fixed FAP, subject to the constraint that it uses only cross-correlations between pulsars. Third is the NPMV statistic, which is the quadratic statistic that is ‘‘as close as possible’’ to the Neyman-Pearson-optimal statistic, also under the constraint that it uses only cross-correlations, see (11). In last place is the DFCC or DF statistic, which are identical for the CURN null hypothesis that we consider for our models.

We employ a toy model for the data. This enables the NPCC filter to be found by numerically optimizing the analytical form of F , as obtained in Sec. 6 for a generalized χ^2 distribution. (Note that for realistic data we cannot use the analytical form (49) and (50), because the data cannot be described in terms of a complex-valued random process.)

7.1. Toy Model

Our synthetic PTA contains $n = 67$ pulsars whose sky locations are chosen to match the NANOGrav 15-year data set (Agazie et al. 2023a). The direction to each pulsar on the sky is represented by a unit vector \hat{n}_a , where the index $a = 1, \dots, n$ labels the pulsars. For each pulsar, the data consists of a single complex number z_a . The full dataset is represented as an n -dimensional column vector z , whose components are the individual z_a .

For the signal hypothesis H_S , the z are described by a zero-mean complex normal distribution

$$z \sim \mathcal{CN}(0, \mathbf{C}), \quad (51)$$

with a real covariance matrix

$$\mathbf{C} \equiv \kappa^2 \mu_{ab} + \sigma^2 \delta_{ab}. \quad (52)$$

The pulsar noise variance is $\sigma^2 = 1$ and the GWB variance is $\hat{\kappa}^2 = 1$. The HD matrix is

$$\mu_{ab} \equiv \frac{1}{2}(1 + \delta_{ab}) - \frac{1}{8}(1 - \hat{n}_a \cdot \hat{n}_b) + \frac{3}{4}(1 - \hat{n}_a \cdot \hat{n}_b) \log \left(\frac{1 - \hat{n}_a \cdot \hat{n}_b}{2} \right). \quad (53)$$

Note that this is often written in terms of $\cos \gamma_{ab} = \hat{n}_a \cdot \hat{n}_b$, where γ_{ab} is the angle between the lines of sight to pulsars a and b .

For the null hypothesis H_0 , we use CURN as discussed in Sec. 4.1. The H_0 data are described by $z \sim \mathcal{CN}(0, \text{Diag } \mathbf{C})$, so the noise covariance is $\mathbf{N} = \text{Diag } \mathbf{C}$ as given in (14). This CURN hypothesis preserves the GWB induced autocorrelations, but eliminates the HD cross-correlations. It is considered “more conservative” than the alternative, which would be to set $\hat{\kappa} = 0$ in (52) giving $\mathbf{N} \equiv N_{ab} = \sigma^2 \delta_{ab}$.

7.2. ROC curves for Toy Model

For the toy model, we form the DFCC, NP, and NPMV filters as in (8), (10), and (12). To construct the NPCC filter, we solve the full numerical optimization problem, maximizing the detection probability at fixed FAP, using the exact expressions for the CDF in (49) and (50). This is a demanding task: the objective function is high-dimensional and strongly multi-modal, with a large region of parameter space whose attraction basins pull the optimization towards the DFCC filter. In practice, we find that from generic initial conditions, many optimizers converge to DFCC rather than to the desired cross-correlation NPCC solution.

To overcome this unwanted convergence to DFCC, we employ an ensemble search strategy, combining the stochastic *simultaneous perturbation stochastic approximation* (SPSA) method (Spall 1998)—whose stochastic updates resemble an annealing process—with subsequent local refinement using the derivative-free BOBYQA algorithm (Powell 2009). By launching many such searches from diverse starting points, and in particular from the vicinity of the NPMV filter, we consistently find solutions whose ROC curves lie above those of NPMV. This demonstrates that the true NPCC filter is close to NPMV in form but achieves higher detection probability. Although we cannot guarantee convergence to the unique global maximum, the consistency of our toy model results across independent ensemble runs indicates that we are closely approaching the genuine NPCC solution.

The ROC curves of the various different detection statistics are shown in Fig. 2.

7.3. ROC curves for more realistic model

To compare the different detection statistics in a more realistic setting, we use the published NANOGrav 15-year “fixed-

γ ” signal and pulsar noise parameter model values⁵ (as used in Fig. 1c of Agazie et al. 2023a), with $A_{\text{gw}} = 2.1 \times 10^{-15}$ and spectral index $\gamma = 13/3$ for the GWB. The amplitude A_{gw} and spectral index γ are related to the dimensionless energy-density spectrum $\Omega_{\text{gw}}(f)$ of the GWB via

$$\Omega_{\text{gw}}(f) = \frac{2\pi^2}{3H^2} A_{\text{gw}}^2 f_{\text{yr}}^2 \left(\frac{f}{f_{\text{yr}}} \right)^{5-\gamma}. \quad (54)$$

Here, $H \approx 70 \text{ km s}^{-1} \text{ Mpc}^{-1}$ is the present-day Hubble constant, and $f_{\text{yr}} \equiv 1/\text{yr}$ [see e.g., Sec. 2.5 in (Romano & Cornish 2017)].

We construct ROC curves for the different quadratic detection statistics. We form the NP and NPMV statistics for realistic data using (20) and (21). These plots of detection probability versus FAP are shown in Fig. 3. At the discovery $5\text{-}\sigma$ threshold FAP of 2.9×10^{-7} , the NPMV statistic results in a 47% increase in detection probability compared to the standard deflection-optimal statistic. The Neyman-Pearson statistic NP has the best performance (highest detection probability), but it is not robust because it makes use of autocorrelations.

8. CONCLUSION

This paper introduces a new quadratic detection statistic for pulsar timing arrays (PTA), which we call the “Neyman-Pearson-Minimum-Variance” statistic and denote with NPMV. We argue that the NPMV statistic should replace the traditional “optimal” cross-correlation detection statistic, which we denote by DFCC, and which is currently used by all of the PTA collaborations to assess their false alarm probabilities (FAPs) and p -values.

Like DFCC, the NPMV statistic uses only pulsar cross-correlations, making it robust against uncertainties in pulsar timing residual noise modeling. But the NPMV statistic has a significant advantage over DFCC: at a given FAP, it is more sensitive. In simulations that model the current generation of PTAs, NPMV has a 47% higher detection probability than DFCC, when operating at the 5σ -equivalent FAP of 2.9×10^{-7} .

The related NPCC statistic is guaranteed to perform even better than NPMV. However, it can only be obtained numerically, and our investigations indicate that in practice it only provides modest improvements over NPMV.

The NPMV filter is implemented in the `enterprise_extensions` package (Ellis et al. 2020; Taylor et al. 2021). This means that existing analyses based on the DFCC statistic can be easily redone using the NPMV detection statistic.

⁵ Exact values of the noise parameters can be found at: https://github.com/nanograv/15yr_stochastic_analysis/blob/main/tutorials/data/optstat_ml_gamma4p33.json.

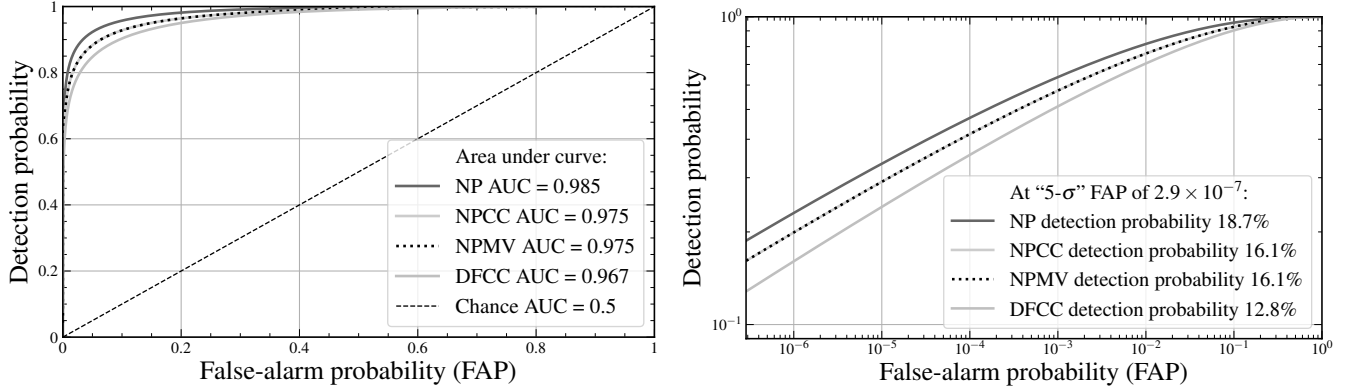


Figure 2. ROC curves of different detection statistics, for the toy model of Sec. 7.1. These compare the standard “optimal” cross-correlation deflection statistic DFCC, the Neyman-Pearson-optimal statistic NP, the cross-correlation-only Neyman-Pearson statistic NPCC, and the cross-correlation-only Neyman-Pearson-Minimum-Variance statistic NPMV. Left panel: linear scale. Legend gives AUC “area under the ROC curve” for the different statistics (larger is better). Right panel: same as left panel, but for logarithmic axes. Legend gives detection probability for the different statistics at the 5- σ discovery threshold FAP of 2.9×10^{-7} (leftmost plot boundary).

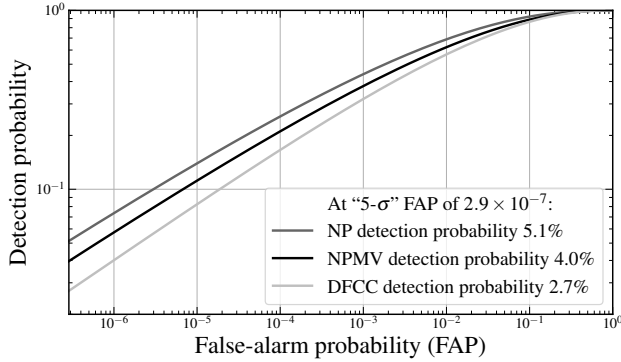


Figure 3. ROC curves for the DFCC, NP, and NPMV detection statistics, for the NANOGrav 15-year PTA fixed $\gamma = 13/3$ GWB and pulsar noise model (Agazie et al. 2023a). At the discovery threshold FAP of 2.9×10^{-7} (leftmost plot boundary) the NPMV statistic increases the detection probability by $\sim 47\%$ compared to the currently-standard “optimal” cross-correlation detection statistic DFCC.

ACKNOWLEDGMENTS

- 1 We thank Wang-Wei Yu for helpful discussions. J.D.R. acknowledges financial support from NSF Physics Frontier Center Award PFC-2020265 and start-up funds from the University of Texas Rio Grande Valley. J.D.R. performed part of this work at the Aspen Center for Physics, which is supported by National Science Foundation grant PHY-2210452.

DATA AVAILABILITY STATEMENT

No open or closed data were used in this work. We make use of pulsar positions and model parameters as described in publications in the literature (Agazie et al. 2023a). All figures can be regenerated using code available online at <https://github.com/vhaasteren/robust-ds-figures>.

REFERENCES

- Afzal, A., Agazie, G., Anumalapudi, A., et al. 2023, The Astrophysical Journal Letters, 951, L11, doi: [10.3847/2041-8213/acdc91](https://doi.org/10.3847/2041-8213/acdc91)
- Agazie, G., Anumalapudi, A., Archibald, A. M., et al. 2023a, The Astrophysical Journal Letters, 951, L8, doi: [10.3847/2041-8213/acdac6](https://doi.org/10.3847/2041-8213/acdac6)
- . 2023b, The Astrophysical Journal Letters, 951, L50, doi: [10.3847/2041-8213/ace18a](https://doi.org/10.3847/2041-8213/ace18a)
- . 2024, The NANOGrav 15 Yr Data Set: Posterior Predictive Checks for Gravitational-Wave Detection with Pulsar Timing Arrays, arXiv, doi: [10.48550/arXiv.2407.20510](https://doi.org/10.48550/arXiv.2407.20510)
- Allen, B. 2023, Physical Review D, 107, 043018, doi: [10.1103/PhysRevD.107.043018](https://doi.org/10.1103/PhysRevD.107.043018)
- Allen, B., Dhurandhar, S., Gupta, Y., et al. 2023, The International Pulsar Timing Array Checklist for the Detection of Nanohertz Gravitational Waves, arXiv, doi: [10.48550/arXiv.2304.04767](https://doi.org/10.48550/arXiv.2304.04767)
- Allen, B., & Romano, J. D. 2023, Physical Review D, 108, 043026, doi: [10.1103/PhysRevD.108.043026](https://doi.org/10.1103/PhysRevD.108.043026)
- . 2024, Optimal Reconstruction of the Hellings and Downs Correlation, arXiv, doi: [10.48550/arXiv.2407.10968](https://doi.org/10.48550/arXiv.2407.10968)
- Anholm, M., Ballmer, S., Creighton, J. D. E., Price, L. R., & Siemens, X. 2009, Physical Review D, 79, 084030, doi: [10.1103/PhysRevD.79.084030](https://doi.org/10.1103/PhysRevD.79.084030)
- Antoniadis, J., Arumugam, P., Arumugam, S., et al. 2023, Astronomy & Astrophysics, 678, A49, doi: [10.1051/0004-6361/202346842](https://doi.org/10.1051/0004-6361/202346842)

- . 2024a, *Astronomy & Astrophysics*, 685, A94, doi: [10.1051/0004-6361/202347433](https://doi.org/10.1051/0004-6361/202347433)
- . 2024b, *Astronomy & Astrophysics*, 690, A118, doi: [10.1051/0004-6361/202348568](https://doi.org/10.1051/0004-6361/202348568)
- Chamberlin, S. J., Creighton, J. D. E., Siemens, X., et al. 2015, *Physical Review D*, 91, 044048, doi: [10.1103/PhysRevD.91.044048](https://doi.org/10.1103/PhysRevD.91.044048)
- Cox, D. 1962, *Renewal Theory*, 1st edn., Methuen's Monographs on Applied Probability and Statistics (London: Methuen)
- Das, A., & Geisler, W. S. 2021, *Journal of Vision*, 21, 1, doi: [10.1167/jov.21.10.1](https://doi.org/10.1167/jov.21.10.1)
- Ellis, J. A., Siemens, X., & van Haasteren, R. 2013, *The Astrophysical Journal*, 769, 63, doi: [10.1088/0004-637X/769/1/63](https://doi.org/10.1088/0004-637X/769/1/63)
- Ellis, J. A., Vallisneri, M., Taylor, S. R., & Baker, P. T. 2020, ENTERPRISE: Enhanced Numerical Toolbox Enabling a Robust Pulsar Inference Suite, Zenodo, doi: [10.5281/zenodo.4059815](https://doi.org/10.5281/zenodo.4059815)
- Hazboun, J. S., Meyers, P. M., Romano, J. D., Siemens, X., & Archibald, A. M. 2023, *Phys. Rev. D*, 108, 104050, doi: [10.1103/PhysRevD.108.104050](https://doi.org/10.1103/PhysRevD.108.104050)
- Hellings, R. W., & Downs, G. S. 1983, *The Astrophysical Journal*, 265, L39, doi: [10.1086/183954](https://doi.org/10.1086/183954)
- Horn, R. A., & Johnson, C. R. 2012, *Matrix Analysis*, 2nd edn. (Cambridge, UK: Cambridge University Press), doi: [10.1017/CBO9781139020411](https://doi.org/10.1017/CBO9781139020411)
- Isserlis, L. 1918, *Biometrika*, 12, 134, doi: [10.1093/biomet/12.1-2.134](https://doi.org/10.1093/biomet/12.1-2.134)
- Powell, M. J. D. 2009, The BOBYQA algorithm for bound constrained optimization without derivatives, Technical Report DAMTP 2009/NA06, University of Cambridge, Cambridge. http://www.damtp.cam.ac.uk/user/na/NA_papers/NA2009_06.pdf
- Rasmussen, C. E., & Williams, C. K. 2006, *Gaussian Processes for Machine Learning* (MIT Press)
- Reardon, D. J., Zic, A., Shannon, R. M., et al. 2023, *The Astrophysical Journal Letters*, 951, L6, doi: [10.3847/2041-8213/acdd02](https://doi.org/10.3847/2041-8213/acdd02)
- Romano, J. D., & Cornish, Neil. J. 2017, *Living Reviews in Relativity*, 20, 2, doi: [10.1007/s41114-017-0004-1](https://doi.org/10.1007/s41114-017-0004-1)
- Spall, J. 1998, *IEEE Transactions on Aerospace and Electronic Systems*, 34, 817, doi: [10.1109/7.705889](https://doi.org/10.1109/7.705889)
- Taylor, S. R., Baker, P. T., Hazboun, J. S., & Simon, J. 2021, *Enterprise_extensions*
- Vallisneri, M., Meyers, P. M., Chatziioannou, K., & Chua, A. J. K. 2023, *Physical Review D*, 108, 123007, doi: [10.1103/PhysRevD.108.123007](https://doi.org/10.1103/PhysRevD.108.123007)
- van Haasteren, R. 2025, On the Calculation of P-Values for Quadratic Statistics in Pulsar Timing Arrays, arXiv, doi: [10.48550/arXiv.2506.10811](https://doi.org/10.48550/arXiv.2506.10811)
- van Haasteren, R., & Vallisneri, M. 2014, *Physical Review D*, 90, 104012, doi: [10.1103/PhysRevD.90.104012](https://doi.org/10.1103/PhysRevD.90.104012)
- Vigeland, S. J., Islo, K., Taylor, S. R., & Ellis, J. A. 2018, *Physical Review D*, 98, 044003, doi: [10.1103/PhysRevD.98.044003](https://doi.org/10.1103/PhysRevD.98.044003)
- Xu, H., Chen, S., Guo, Y., et al. 2023, *Research in Astronomy and Astrophysics*, 23, 075024, doi: [10.1088/1674-4527/acdfa5](https://doi.org/10.1088/1674-4527/acdfa5)